

Mass spectrometric analysis of 7-sulfoxymethyl-12-methylbenz[*a*]anthracene and related electrophilic polycyclic aromatic hydrocarbon metabolites

Andreas F. Lehner,^{1*} Jamie Horn² and James W. Flesher²

¹ Department of Veterinary Science, University of Kentucky, Maxwell H. Gluck Equine Research Center, Lexington, Kentucky 40546, USA

² Experimental Cancer Research Laboratory, Department of Pharmacology, University of Kentucky, Lexington, Kentucky 40536, USA

Received 27 May 2004; Accepted 9 July 2004

The Meso-region theory of polycyclic aromatic hydrocarbon (PAH) carcinogenesis predicts that the development of pronounced carcinogenicity depends on the introduction of a good leaving group on alkyl side-chains attached to the exceptionally reactive meso-anthracenic or L-region positions of PAHs. Thus, the first step in carcinogenesis by methylated PAHs such as 7,12-dimethylbenz[*a*]anthracene (DMBA) would be the hydroxylation of the L-region methyl groups, particularly the 7-methyl group. The second would be the formation of a metabolite, e.g. a sulfate ester, which is expected to be a good leaving group capable of generating a highly reactive benzylic carbocation. 7-Hydroxymethyl-12-methylbenz[*a*]anthracene (7-HMBA) is a metabolite of DMBA, and sulfation of 7-HMBA to a 7-sulfoxymethyl metabolite (7-SMBA) is a known Phase II metabolic process designed to facilitate excretion, but actually enabling more destructive side-reactions. These side-reactions occur with generation of an electrophilic 7-methylene carbonium ion, and/or by *in vivo* halide exchange to provide neutral side-products more capable of entering cells, especially those of DMBA target tissues. Electrospray ionization mass spectrometry (MS) enabled us to visualize 7-SMBA as an intact *m/z* 351 conjugate anion by negative mode, and as a released *m/z* 255 carbonium ion by positive mode. Upon prolonged refrigeration, 7-SMBA accumulated an *m/z* 383 photoxide, which appeared capable of re-evolving the starting material as visualized by tandem quadrupole MS, or MS/MS. The 7-SMBA carbonium ion provided interpretable fragments when studied by fragment ion MS/MS, including those representing the loss of up to several protons. Subtle differences in this property were encountered upon perturbing 7-SMBA, either by warming it at 37 °C for 2 h or by substituting the initial sulfoxy group with an iodo group. Side-reactions accounting for such proton losses are proposed, and are of interest whether they occur in the mass spectrometer, in solution or both; these proposals include acidity at the 12-methyl position and cyclization between the 12-methyl group and the adjacent C-1 position. It is also suggested that such side-reactions may comprise one route to relieving steric strain arising between the 12-methyl group and the angular benzo ring of 7-SMBA. Copyright © 2004 John Wiley & Sons, Ltd.

KEYWORDS: Meso-region theory; sulfated carcinogens; activation; polycyclic aromatic hydrocarbons

INTRODUCTION

Carcinogenesis by polycyclic aromatic hydrocarbons (PAHs) has long been suspected to depend on the metabolic introduction of specific functional groups in the PAH structure. One well-established description of such proposed metabolism, the Meso-region theory of PAH carcinogenesis, predicts that the development of complete carcinogenic properties depends on the occurrence of one or more substitution reactions culminating in the introduction of a good leaving group on alkyl side-chains attached to reactive meso-anthracenic or L-region positions.^{1,2} According to this theory, substitution with specific groups that happen

to be excellent leaving groups can lead to the development of stable reactive carbonium ions, which, as electrophilic intermediates, can react with cellular nucleophilic targets including DNA, resulting in mutation.^{2–5} This theoretical pathway is summarized in Fig. 1 for the well-characterized carcinogen 7,12-dimethylbenz[*a*]anthracene (DMBA), illustrating hydroxyl substitution on the 7-methyl position via cellular cytochrome P450 enzymes, followed by sulfate substitution on the hydroxyl group catalyzed by sulfotransferase enzymes. The sulfate is a good leaving group that departs efficiently while generating highly reactive benzylic carbonium ions capable of introducing lesions in cellular DNA. As shown in Fig. 1, 7-sulfoxymethyl-12-methylbenz[*a*]anthracene (7-SMBA) can also undergo exchange of the sulfate group with halide anions to give 7-chloro-, -bromo- or -iodomethyl-12-methylBA. The synthetic route to 7-SMBA is also summarized in Fig. 1.

*Correspondence to: Andreas F. Lehner, Department of Veterinary Science, University of Kentucky, Maxwell H. Gluck Equine Research Center, Lexington, Kentucky 40546, USA.
E-mail: alehner@uky.edu

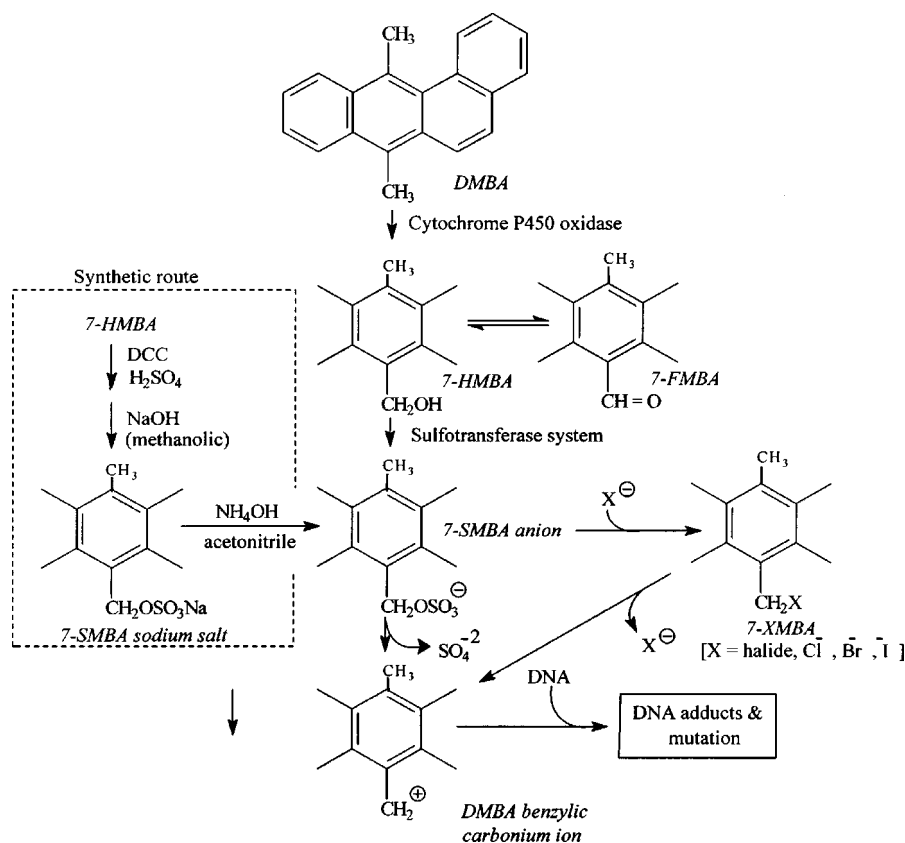


Figure 1. Central scheme for the Meso-region theory of PAH carcinogenesis as illustrated with 7,12-dimethylbenz[a]anthracene (DMBA). The 7-methyl group is hydroxylated by cytochrome P450 enzymes to give 7-hydroxymethyl-12-methylBA (7-HMBA). This compound is capable of oxidizing further to 7-formyl-12-methylBA (7-FMBA), which is capable of reduction back to 7-HMBA presumably by cellular keto–aldo reductases.⁵² 7-HMBA is subject to cellular sulfotransferase enzymes, coupling via esterification with sulfate to give 7-sulfoxymethyl-12-methylBA (7-SMBA anion).^{7,10,53} Release of sulfate generates a benzylic carbonium ion capable of reacting with sensitive nucleophiles such as DNA.⁴⁰ 7-SMBA can also undergo exchange of the sulfate group with halide anions to give 7-chloro-, -bromo- or -iodomethyl-12-methylBA.^{8,21} The synthetic scheme for 7-SMBA sodium salt is shown starting from 7-HMBA in 0 °C DMF with 5 × dicyclohexylcarbodiimide (DCC) plus 1.5 × H₂SO₄. The product was neutralized with 1 M methanolic NaOH, dried, dissolved in DMF–ethanol (1 : 1), precipitated with excess 0 °C diethyl ether and dried.¹⁰ The 7-SMBA anion was then generated for ESI(–)–MS characterization from a methanolic solution by dilution in 0.5% ammonium hydroxide–acetonitrile (1 : 1). Note: six-membered ring representations are abbreviations of changes specific to the DMBA meso ring.

Metabolic routes to the introduction of good leaving groups include aspects of Phase II metabolism of xenobiotics, which often add bulky water-soluble groups (glucuronic acid, glycine, sulfate, etc.) to drugs, steroids, toxins and so forth, in many cases following Phase I hydroxylations. Such groups generally have the chemical property of facilitating excretion via the kidney or liver.⁶ However, these water-soluble groups also occasionally have the property of functioning as excellent leaving groups, and Phase II metabolic conjugates considered by the Meso-region theory include the sulfate esters,⁷ in addition to phosphates and acetates. Spontaneous substitution of any of these with halides also provides good leaving group potential.⁸ Glucuronides, glutathione conjugates and mercaptides are less likely to be good leaving groups should they form, and in general would be the preferred conjugates from the viewpoint of thwarting the potentially damaging effects of reactive electrophilic species.

This paper presents the mass spectrometric characterization of the recently synthesized 7-sulfoxymethyl-12-methylbenz[a]anthracene, an ultimate electrophilic and

strongly carcinogenic form of the proximate carcinogen 7-SMBA. In addition, we show various chemical properties as revealed spectrometrically, and also those of related halogenated compounds.

EXPERIMENTAL

7-Hydroxymethyl-12-methylbenz[a]anthracene (7-HMBA)

7-HMBA was prepared as described previously in detail by Flesher *et al.*⁹

7-Sulfoxymethyl-12-methylbenz[a]anthracene (7-SMBA)

The sodium salt of 7-SMBA was synthesized according to the synthetic scheme appended to Fig. 1.¹⁰ 7-SMBA (47 mg, 126 μmol; 63% yield) was synthesized from 7-HMBA (54 mg, 199 μmol) by a 1 h reaction with 1.5 × H₂SO₄ in the presence of a fivefold molar excess of dicyclohexylcarbodiimide (DCC; 205 mg, 993 μmol) at 0 °C in dimethylformamide

(DMF) (7 ml). The product was neutralized with 1 M methanolic NaOH, dried, dissolved in 1:1 DMF–ethanol (1 ml), precipitated with a 10× volume of diethyl ether at 0 °C and dried. The resulting compound was recrystallized and found to be pure by HPLC analysis, and reasonably stable upon storage at –80 °C in the dark.¹⁰

7-Iodomethyl-12-methylbenz[*a*]anthracene (7-IMBA)

7-IMBA was synthesized according to the method of Sandin and Fieser.¹¹ A Grignard reagent was formed from the reaction of Mg (1 g, 42 mmol) and excess methyl iodide (7 ml) in anhydrous diethyl ether (20 ml). After all the Mg had been consumed, a solution of benzantraquinone (1 g, 4 mmol) in benzene (20 ml) was added slowly with stirring and heating. The reaction mixture was refluxed for 40 min and allowed to react for a further 3 h at room temperature. The mixture was then poured slowly, with vigorous stirring, into a solution of hydroiodic acid (12 ml) and methanol (40 ml) at –10 °C. Glacial acetic acid (40 ml) was added to aid in the precipitation of the bright yellow iodomethyl compound. The product was dried under vacuum and stored at 0 °C in the dark.

7-Chloromethyl-12-methylbenz[*a*]anthracene (7-CMBA)

The synthesis of 7-CMBA was carried out following the procedure of Pataki *et al.*¹² Thionyl chloride (1 ml, 14 mmol) was added to a solution of 7-HMBA (1 g, 4 mmol) in benzene (20 ml). The reaction mixture was refluxed for 30 min under N₂ and then dried under reduced pressure. Addition of hot benzene to the resulting residue resulted in the crystallization of the 7-chloromethyl product.

7-Chloromethylbenz[*a*]anthracene (7-CBA)

7-CBA was prepared in essentially the same manner as 7-CMBA, by utilization of 7-hydroxymethylbenz[*a*]anthracene as the starting material.

Electrospray ionization mass spectrometry (ESI-MS)

Compounds were prepared as 1 mg ml⁻¹ solutions in methanol then immediately diluted 1:100 with 0.5% ammonium hydroxide–acetonitrile (1:1) for direct infusion ESI (negative or positive mode) MS analysis. Infusion was carried out with a Harvard (Holliston, MA, USA) syringe pump equipped with a 500 µl Hamilton gas-tight syringe. The mass spectrometer was a Micromass (Beverly, MA, USA) Quattro II tandem quadrupole instrument capable of atmospheric pressure ionization, and typical ESI-MS voltage settings and conditions for detection and analysis of sulfate esters by negative mode were as follows: capillary, 3.4 kV; HV lens, 0.66 kV; cone, 30 V; skimmer lens, 1.9 V; r.f. lens, 0.0 V; source temperature, 100 °C; argon pressure for collisionally induced dissociation (CID) experiments, 6 × 10⁻⁴ mbar; and ionization energies, MS1 1.7 V and MS2 2.0 V. Regular, parent and fragment ion scans were generally acquired over an *m/z* range of 50–500 at 2.96 s per scan with a 0.1 s reset time. Direct infusion spectra were generated over a minimum 1–2 min acquisition time. Spectra were interpreted with the

assistance of Mass Spec Calculator Pro software, version 4.03 (Quadtech Associates, 1998; published by ChemSW, Fairfield, CA, USA).

Gas chromatographic/mass spectrometric (GC/MS) analysis

Injection of dichloromethane-dissolved compounds at 10 µg ml⁻¹ or less was made through the 250 °C injector port of an Agilent (Palo Alto, CA, USA) 6890/5972 GC/MSD system, a single-quadrupole instrument, with sample deposition onto a 30 m × 0.25 mm i.d., 0.25 µm film thickness, DB-5MS 5% phenyl–95% methylpolysiloxane column (J&W Scientific, Folsom, CA, USA) with oven programming beginning at 70 °C (held for 2 min), then ramped at 20 °C min⁻¹ to 280 °C (held for 12 min). The mass spectrometer was set up to acquire from *m/z* 50 to 550 at 1.53 scans s⁻¹ with a threshold of 150.

Hyperchem

Molecular geometries were optimized by semi-empirical AM1 calculation with Hyperchem Release 3 (Hypercube, Gainesville, FL, USA, 1993).

RESULTS

Synthetic 7-SMBA was demonstrated to be reasonably pure (>95%) by HPLC,¹⁰ with fluorescence detection revealing no 7-HMBA starting material (data not shown). ESI-MS negative mode (ESI(–)-MS) analysis was considered a useful tool owing to the anticipated sulfate functionality and its anionic character at high pH. Examination of 7-SMBA by direct infusion ESI(–)-MS revealed a large peak at *m/z* 351 (Fig. 2(A)), corresponding to the intact sulfate ester anion with reasonable isotopic abundances at *m/z* 352 and 353 that matched those of the expected product. An MS/MS fragment ion spectrum generated from the *m/z* 351 [M – H]⁻¹ pseudomolecular ion is shown in Fig. 2(B). Reasonable assignments based on mass could be made to the resultant fragments in accordance with the anticipated structure, as listed in the caption to Fig. 2; Fig. 2(C) displays cleavages to principal fragments. For example, *m/z* 271 results from a loss of neutral SO₃, whereas loss of CH₂OSO₃ from the 7-position gives *m/z* 241. Ions at *m/z* 96 and 81 correspond to formulas SO₄ and HSO₃, respectively. Fragments in the vicinity of *m/z* 253, 3 Da less than the presumed demethylated oxymethyl anion at *m/z* 256, provided an interesting story which gradually revealed itself during other facets of our study and which is discussed in greater detail below.

Preparations of 7-SMBA stored for months at –80 °C generally acquired a contaminant revealed as an *m/z* 383 peak that was assigned the identity 7-SMBA photooxide after direct infusion ESI(–)-MS analysis. Figure 3(A) reveals ESI(–)MS/MS parent ion scan evidence of such a contaminant; *m/z* 383 was found to be the only ion acting as an *m/z* 351 precursor. Figure 3(B) shows the *m/z* 383 fragment ion spectrum, which contains most of the significant 7-SMBA fragment ions (compare Fig. 2(B)) including *m/z* 81, 96, 241, 271 and most notably 351, implying both a direct derivation

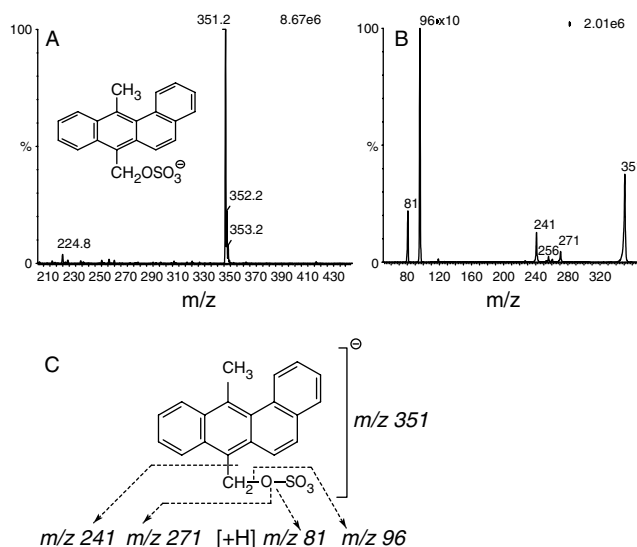


Figure 2. 7-SMBA analyzed by direct infusion ESI(-)-MS/MS. The compound was dissolved at $10 \mu\text{g ml}^{-1}$ in 0.5% NH_4OH -acetonitrile (1 : 1) and infused at 1.2 ml h^{-1} . (A) Full-scan analysis with inset structure of expected compound ($\text{C}_{20}\text{H}_{15}\text{O}_4\text{S}_1$, 351 monoisotopic M_r as anion); isotopic analysis of $M - H$, $M - H + 1$, $M - H + 2$ and $M - H + 3$ showed the following relative amounts (parenthetical values predicted): m/z 351, 100%; m/z 352, 23.2% (23.4); m/z 353, 8.4% (7.7); m/z 354, 1.7% (1.0). (B) Fragment ion analysis of m/z 351, with m/z 110–310 region enhanced 10-fold. Peak assignments: m/z 351 = $M - H$; m/z 271 = loss of SO_3 ; m/z 256 = m/z 271 minus CH_3 ; m/z 241 = loss of CH_2OSO_3 ; m/z 96 = SO_4^- ; m/z 81 = HSO_3^- . (C) Fragmentation scheme to principal 7-SMBA fragment ion peaks.

of m/z 383 from 7-SMBA and the ability to regenerate the starting material. Owing to the 32 Da difference between this contaminant and 7-SMBA, we proposed the photooxide as arising by a series of single electron migrations as described in the Fig. 3(C) reaction scheme and implicating interaction with singlet diradical O_2 . In addition to bridging the 7,12-positions, other potential photooxide bridges could also be postulated across the open 1,4- and 8,11-positions. Greater electron density calculated by the Hyperchem AM1 semi-empirical method for the 1-, 4-, 8- and 11-positions relative to the 7,12-positions disclosed deficiency of electron density at positions 7 and 12; this is in agreement with Klein *et al.*,¹³ who noted that these positions are highly reactive, and therefore the fragment ion spectrum could be reasonably assigned to the structure in Fig. 3(C). Figure 3(D) includes an interpretation of m/z 383 fragment ions consistent with fragmentations observed for the starting material in Fig. 2. Note the differences from 7-SMBA induced by the 7,12-bicyclic peroxy function, particularly the new abilities to discharge a naphthalenic group as a neutral fragment, as suggested for minor ions m/z 145 and 225 arising by two or more fragmentation events, and the more significant m/z 258 arising by two bond cleavages directly from the parent ion, and the ability of CH_2SO_4 to depart bearing a negative charge. Negative mode parent ion analysis established the m/z 383/351 precursor/product relationship, as seen

in Fig. 3(A). The m/z 383 ion (7-SMBA photooxide anion in an older preparation for which the initial MS scan disclosed $\sim 5\%$ m/z 383 ion relative to m/z 351) was revealed as precursor with its abundance increasing in proportion to the collision energy setting in the intermediate argon-filled hexapole of the tandem quadrupoles during MS/MS parent ion scanning for m/z 351 precursor(s) under increasing collision energies. This contrasted with the ion at m/z 351 (7-SMBA anion)—acting as its own precursor—which first rose, then fell with increasing collision energy under the same conditions, presumably owing to excessive fragmentation of this ion (data not shown). These non-parallel relationships suggested that the presence of the photooxide was not an instrument-derived artifact.

Positive mode ESI-MS (ESI(+)-MS) analysis of 7-SMBA revealed predominantly an m/z 255 ion, the predicted mass of a positively charged carbonium ion released by simple cleavage of the 7-SMBA C—O bond, releasing HSO_4^- or SO_4^{2-} as its leaving group depending on the extent of protonation (Fig. 4(A)). Isotopic abundance analysis of peaks adjacent to m/z 255 revealed responses reasonably close to the predicted pattern for $\text{C}_{20}\text{H}_{15}$ (Fig. 4(B)), supporting its structural assignment. The observation that 7-SMBA gives rise to a benzylic cationic intermediate (m/z 255) was of considerable interest; although benzylic carbonium ions are common products in mass spectrometric fragmentation, this particular species is a prime candidate for the ultimate electrophilic and carcinogenic form of the proximate carcinogen 7-HMBA¹⁰ and to our knowledge represents its first direct visualization under any conditions.

Various sources in the literature^{14–17} have predicted or ascribed significant instability to the PAH hydroxymethyl sulfate esters, so we decided to investigate the 7-SMBA half-life in unbuffered medium by following the abundance of the m/z 255 carbonium ion in positive mode full-scan spectra by direct infusion ESI-MS. As shown in Fig. 5, room temperature stability was appreciable with a half-life of the order of 22 h. At 37°C the half-life was severely diminished, to a value of the order of 100 min. It would perhaps be advantageous to repeat such studies in different media in future investigations.

ESI(+)-MS fragment ion analysis of the 7-SMBA-derived carbonium ion at m/z 255 revealed an unusual anomaly. A distinct shift in the m/z values of higher molecular mass peaks occurred on mild heating of the preparation. Figure 6 displays fragment ion scans of the m/z 255 ion before and after a 120 min period at 37°C . Prior to heating, the highest m/z fragment ion is 3 Da smaller than the parent at m/z 252, suggesting a capacity for proton loss; heat exposure eliminated the majority of this capability, restricting the principal high-mass peak to the m/z 255 carbonium ion itself.

For comparison, we synthesized and examined 7-iodomethyl-12-methylbenz[*a*]anthracene (7-IMBA), which basically substitutes iodine for 7-SMBA's sulfate leaving group. When 7-IMBA was examined by non-covalent acetate complexation^{18,19} in order to observe this compound directly in the form of a negative ion complex, the compound was instead identified independent of complexation, being revealed instead as a monodeprotonated anion. Figure 7(A)

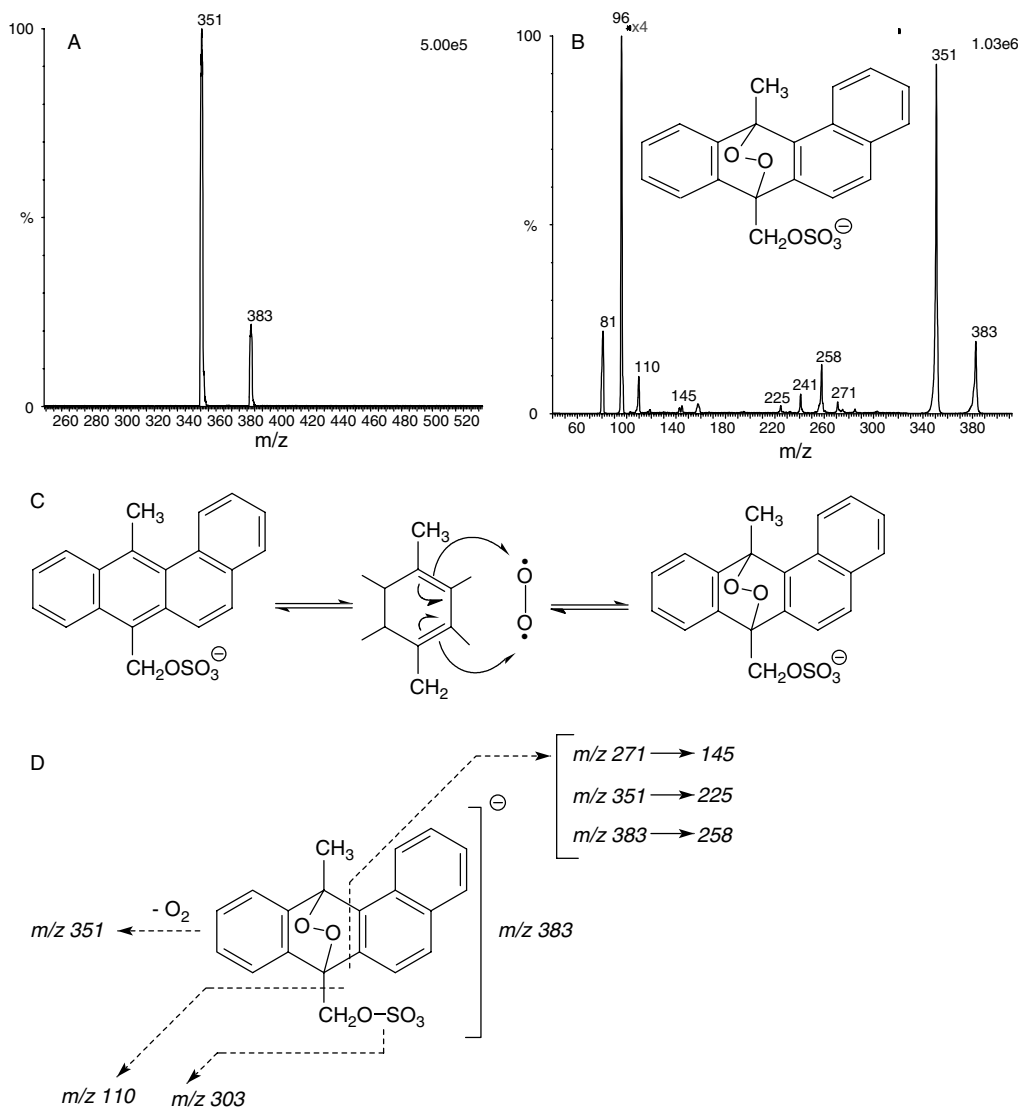


Figure 3. Specific contaminant of 7-SMBA analyzed by direct infusion ESI(-)-MS/MS and assigned as 7-SMBA photooxide. 7-SMBA kept for 1–2 months at -80°C was dissolved at $10\ \mu\text{g ml}^{-1}$ in 0.5% NH_4OH -acetonitrile (1 : 1) and infused at $1.2\ \text{ml h}^{-1}$. (A) Parent ion scan for the m/z 351 ion, indicating a precursor–product relationship for m/z 383 \rightarrow 351 (full-scan results similar, not shown). (B) ESI(-)-MS/MS fragment ion analysis of the m/z 383 contaminant. (C) Proposed photooxide of 7-SMBA, responsible for the m/z 383 contaminant present in preparations of 7-SMBA, indicating a theoretical scheme for its formation from 7-SMBA. Mechanism arrows indicate single electron movements; intermediate addition of intact oxygen could conceivably require more than the single step implied. (D) Fragmentation to major and minor peaks of the 7-SMBA photooxide; other m/z values as assigned to 7-SMBA in Fig. 2, with m/z 241 and 271 after loss of O_2 to give m/z 351.

displays the ESI(-)-MS scan with the principal 7-IMBA peak at m/z 381, 1 Da less than the nominal monoisotopic molecular mass of m/z 382, with no evidence for an m/z 441 acetate complex (neutral monoisotopic M_r 382 + 59 for acetate anion). Figure 7(B) shows the fragment ion spectrum derived from the m/z 381 peak, with the principal fragment at m/z 127, the iodine anion.

Similarly, 7-chloromethyl-12-methylbenz[*a*]anthracene (7-CMBA) and 7-chloromethylbenz[*a*]anthracene (7-CBA) were also identified under the same ESI(-)-MS conditions, but again with no evidence for acetate complexation; these compounds did, however, form complexes with water or with one another following deprotonation, as seen in Fig. 8(A) and (B). 7-CMBA shows an m/z 307 ion, 18 Da greater than an anion anticipated at m/z 289 by analogy

with 7-IMBA, along with an m/z 579 complex, representing the m/z 289 anion combined with an undissociated mass 290 molecule. Similarly, 7-CBA shows an m/z 293 ion, 18 Da greater than an anticipated m/z 275 anion, along with an m/z 551 complex, representing the m/z 275 anion combined with an undissociated mass 276 molecule. The results overall inferred that the property of acidity existed in the group of halo derivatives.

ESI(+)-MS revealed additional findings for the 7-IMBA compound. Figure 9(A) shows an ESI(+)-MS full-scan analysis demonstrating a significant peak at m/z 255, the carbonium ion anticipated from loss of the iodine anion. Reasonable isotopic abundances were obtained for the adjacent m/z 256 and 257 ions, supporting the contention that this was the same structure as released from 7-SMBA (Fig. 4).

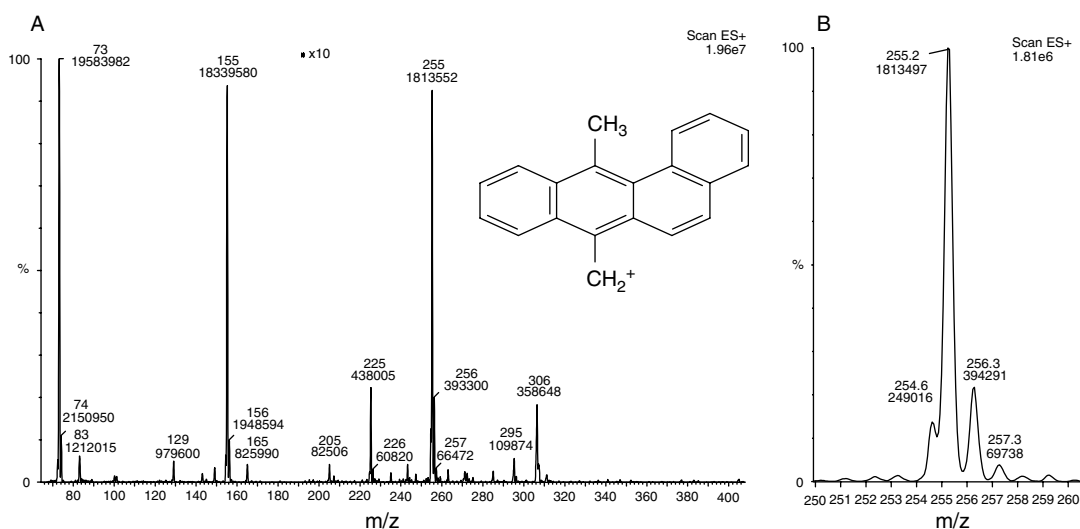


Figure 4. ESI(+) mass spectrum of 7-SMBA diluted from a $20 \mu\text{g ml}^{-1}$ aqueous solution to $10 \mu\text{g ml}^{-1}$ with acetonitrile–0.5% NH_4OH , infused at 1.2 ml min^{-1} . (A) m/z 60–400 scan with 10-fold expansion of ions above $m/z \sim 180$. Ion interpretations: m/z 255 = 7-SMBA carbonium ion; m/z 225 = benz[a]anthracene nucleus; m/z 155 = unknown synthetic contaminant, with no demonstrable origin from higher M_r species according to parent ion analyses (not shown), and demonstrable connection to ions at m/z 73 and 83 by fragment ion analysis, presumably by simple cleavages; m/z 306 is solvent-derived. The structure shown is the principal carbonium ion structure, m/z 255. (B) Distinctive pattern in the vicinity of the 7-SMBA-derived carbonium ion at m/z 255. This ESI(+) spectrum was obtained for 7-SMBA diluted and infused as above. Note the unusual ‘spur’ peak at m/z 254.6. The predicted pattern of peaks in the vicinity of the carbonium ion, with m/z 255.2 at a relative yield of 100%, are as follows: m/z 256.3, predicted 22.5%, found 21.7%; m/z 257.3, predicted 2.3%, found 3.7%.

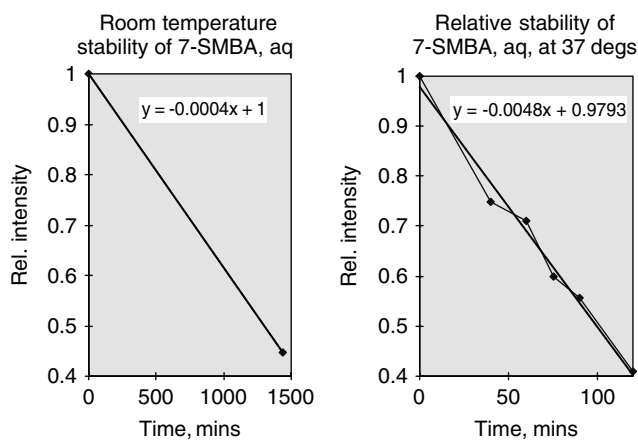


Figure 5. Relative stability of 7-SMBA carbonium ion in unbuffered water + 2% acetonitrile, as measured by its ESI(+)-MS scan intensity: room temperature (left) and 37°C (right). The abundance of the *in situ*-generated [7-SMBA minus HSO_4^-] carbonium ion, m/z 255, was measured by direct infusion ESI(+)-MS. Trendlines derived from Microsoft Excel allowed the estimation of the half-life at 37°C as 100 min and time to disappearance as 204 min.

Fragment ion analysis is shown for the m/z 255 ion (Fig. 9(B)), and the principal high-mass fragment ion peak at m/z 253 was theorized as arising by cyclization between the 12-methyl group and the carbon at the 1-position, accounting for loss of 2 Da as 2H. The inset structure (Fig. 9(B)) shows the carbonium ion product of such an event. Table 1 lists assignments for principal peaks in the fragment ion spectrum of the 7-IMBA-derived carbonium ion, with many of the peaks

Table 1. Interpretation of positive-mode ions generated from the 7-iodomethyl-12-methylbenz[a]anthracene-derived m/z 255 carbonium ion, compared with equivalent spectrum derived from 7-SMBA (the 7-SMBA m/z 255 carbonium ion in addition produced m/z 189, 202 and 250)

Ion (m/z)	Interpretation	How 7-SMBA-derived fragments differed (Da)
253.2	Ring cyclization between 12-methyl and 1-position	-1
239.1	m/z 253.2 minus CH_2	0
227.9	m/z 253.2 minus $\text{CH} \equiv \text{C}$	0
225.8	m/z 253.2 minus $\text{CH}=\text{CH}_2$	0
215.0	m/z 253.2 minus $\text{CH}=\text{C}=\text{CH}_2$	-2
177.4	m/z 253.2 minus C_6H_4	-1
150.9	m/z 253.2 minus $\text{C}_6\text{H}_4-\text{C}-\text{CH}_2$	0
127.1	Naphthalenic residue, C_{10}H_7	0
103.2	$\text{C}_6\text{H}_4-\text{CH}=\text{CH}_2$	-2
76.2	C_6H_4	+1

arising from the m/z 253 intermediate structure. Analysis of the similarly derived 7-SMBA carbonium ion (Fig. 6(B)) gave rise to a spectrum with a very similar appearance, with

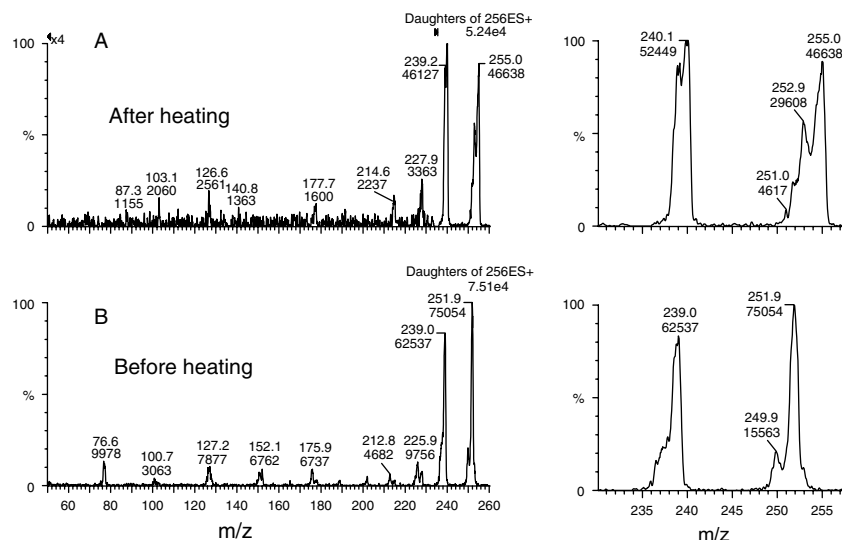


Figure 6. ESI(+) fragment ion mass spectra of the m/z 255.5 carbonium ion from 7-SMBA, run either after (A) or before (B) 120 min at 37 °C. The uppermost figures are post-thermal exposure. Left, m/z 50–260 region; right, expansion of the respective m/z 230–260 region. Note the apparent shift of fragment ion to slightly higher values on heating.

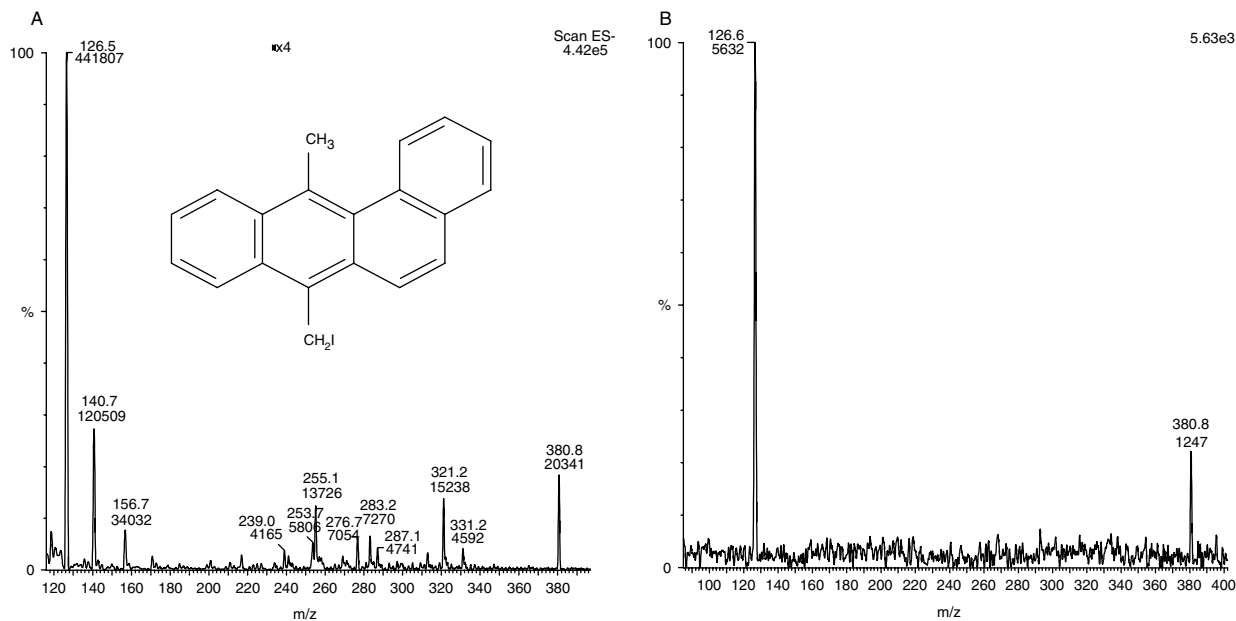


Figure 7. 7-Iodomethyl-12-methylbenz[a]anthracene (monoisotopic M_r 382), $10 \mu\text{g ml}^{-1}$ in 10 mM ammonium acetate–acetonitrile (1 : 1) by direct infusion ESI(-)-MS. (A) Full-scan mode, with vertical scale enhancement between m/z 240 and 400. Peak assignments include m/z 380.8, deprotonated 7-iodomethyl-12-methylBA; m/z 255.1, loss of iodo group; m/z 126.5, iodine anion. The structure shown is the neutral compound, M_r 382. (B) Fragment ion spectrum of the m/z 380.8 peak. Peak assignment: m/z 381, $[\text{M} - \text{H}]^-$; m/z 127, iodine anion.

the exception of several peaks that differ as listed in Table 1, giving a principal high-mass intermediate peak at m/z 252. The subtle differences in the spectra of these compounds suggested slightly differing populations of carbonium ions, poised for self-reaction as revealed by MS/MS.

The proposed cyclization event documented in Fig. 9(B) gained additional support from electron ionization MS studies. The 7-IMBA compound was apparently unstable to thermal volatilization in the 250 °C injector port of the Agilent GC/MS instrument used for its study, giving as a result thermal degradation products separable by GC. The

principal peak was DMBA, M_r 256, monoisotopic, at 16.6 min retention time, as shown in Fig. 10(A), with excellent match to library entries for DMBA. This compound must have arisen by deiodination followed by intermolecular collision and hydrogen abstraction from a second molecule. A minor breakdown peak occurred at 16.7 min retention time, and its mass spectrum is shown in Fig. 10(B); both its monoisotopic molecular mass of 254 and the agreement of its mass spectral peaks with the proposed 1,12-ring cyclized form give support to the Fig. 9(B) structural assignment. Such a compound would then have arisen by sterically induced intramolecular

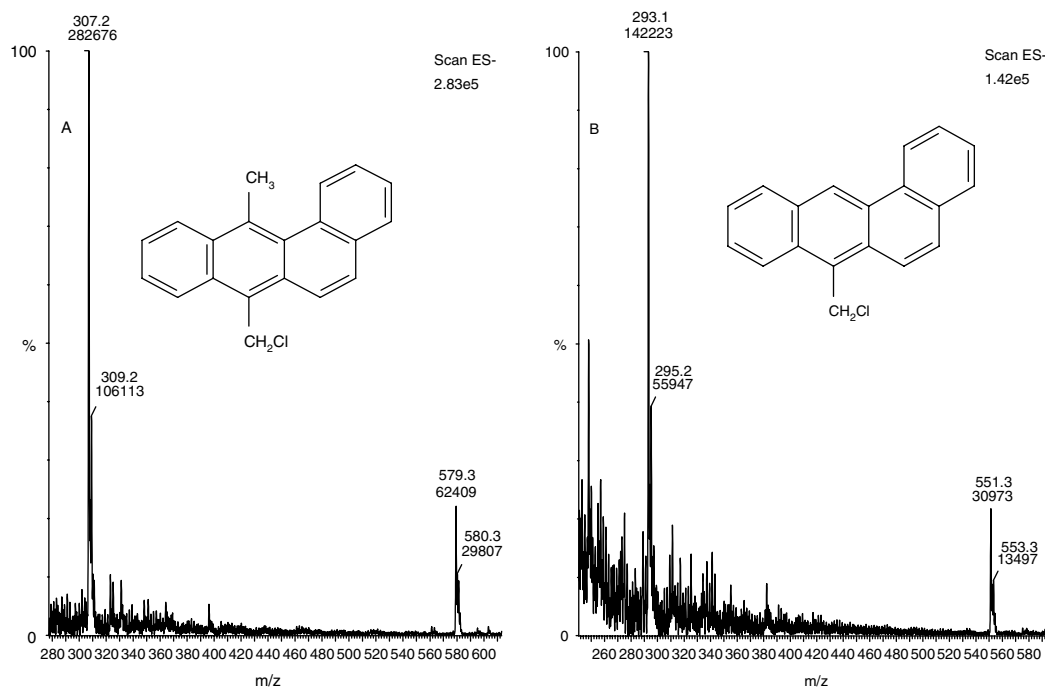


Figure 8. ESI(-)-MS scans of 7-chloromethyl-12-methylbenz[a]anthracene (A) and 7-chloromethylbenz[a]anthracene (B). The structures shown are the neutral compounds studied. Compounds were dissolved at $10 \mu\text{g ml}^{-1}$ in 10 mM ammonium acetate–acetonitrile (1 : 1) (plus 10% DMF), with direct infusion at 1.0 ml h^{-1} for ESI(-)-MS. For peak assignments, see text.

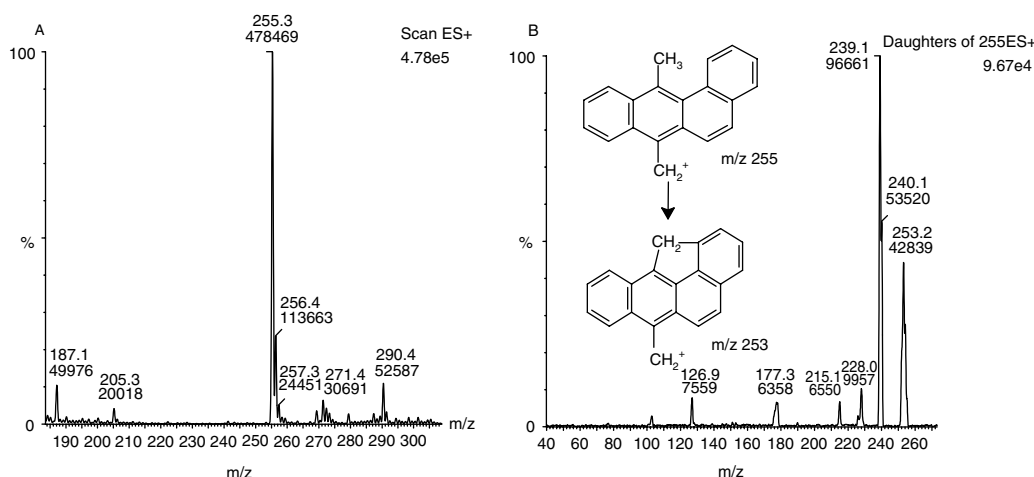


Figure 9. 7-Iodomethyl-12-methylbenz[a]anthracene at $10 \mu\text{g ml}^{-1}$ in 10 mM ammonium acetate–acetonitrile (1 : 1) by direct infusion ESI(+)-MS and -MS/MS. (A) Full-scan mode; the proposed [DMBA minus H] carbonium ion at m/z 255 has adjacent isotopic peaks at m/z 256 (24.3% relative abundance, expected at 22.5%) and m/z 257 (4.6% relative abundance, expected at 2.3%). (B) Fragment ion spectrum of the m/z 255 peak. The structures show the presumed ring-cyclized species corresponding to the principal upfield peak at m/z 253 and its origin from the 7-IMBA m/z 255 carbonium ion.

rearrangement, in contrast to the more abundant DMBA arising by intermolecular hydrogen abstraction.

The results suggested at least two different routes to release of steric strain at the 12-methyl group of DMBA and the related sulfate- or iodo-derived carbonium ions: conformational change and structural rearrangement. The routes were studied by Hyperchem AM1 geometry optimization following molecular modeling as shown in Fig. 11. The top figure reveals strain in DMBA as a 128° methyl C—C-12—C-12a angle between the carbon 12-methyl group and its meso benzo ring, pushing the methyl group away from the angular benzo ring. This contrasts with

the more typical 119° methyl C—C-7—C-6a angle between the methyl at carbon 7 and meso ring in the direction of the K-region (carbons 5 and 6). These findings occur with retention of relative planarity, and disagree with a known propensity for the plane of the rings to twist,²⁰ a result actually obtained with the carbon 7 methylene carbonium ion (Fig. 11, middle) in which methyl-meso ring angles are much less strained. Figure 11 (bottom) shows an optimized structure for the positively charged ring-closed derivative of the Fig. 11 (middle) carbonium ion, affording relief of steric strain at the C-12 methyl group, and based on the C-12—C-1 cyclopenteno derivative originally indicated by the data in

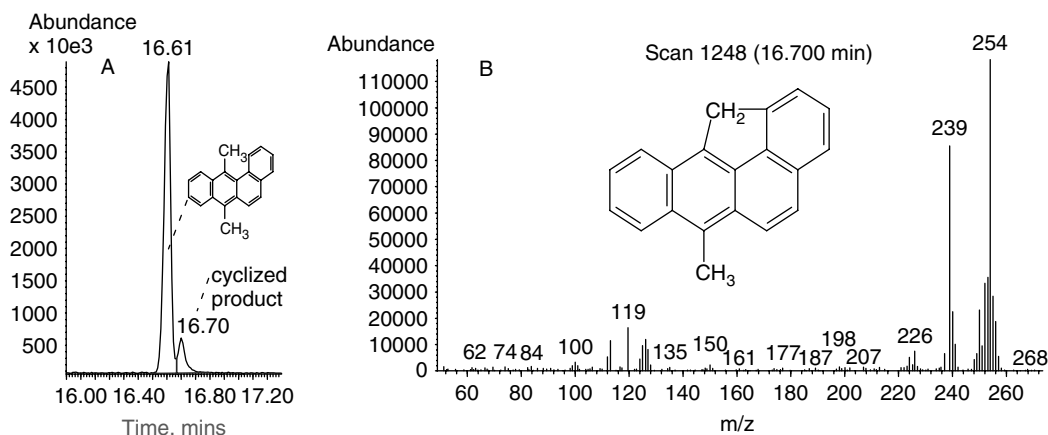


Figure 10. (A) GC/MS analysis of 7-iodomethyl-12-methylBA. Thermal degradation primarily gave the 16.6 min peak identified as DMBA, and arising by intermolecular rearrangement; the smaller 16.7 min peak is a likely ring-cyclized 254 monoisotopic M_r DMBA derivative proposed in the text. (B) EI mass spectrum of the 16.7 min peak; MS Calculator Pro software indicates support for the identification, particularly among the higher masses m/z 254 [$M^{+\bullet}$], 239 [$M^{+\bullet} - \text{CH}_3$] and 226 [$M^{+\bullet} - \text{CH}_2\text{CH}_2$]; the clusters at m/z 113, 119 and 126 must then be doubly charged variants of these, typically found in fully conjugated PAH ring systems.

Fig. 9. Note that the structure bears an initial positive charge at the C-7-methylene, while preserving the overall planarity of DMBA seen in Fig. 11 (top).

DISCUSSION

A fundamental proposition of the Meso-region theory of PAH carcinogenesis is that the development of complete carcinogenic properties depends on the introduction of a good leaving group on the alkyl side-chains attached to the meso-anthracenic or L-region positions of PAHs. Hence the benzylic carbonium ions generated from Phase II metabolism of PAHs such as 7-SMBA,^{1,5,10} or by exchange reactions with halogens such as 7-IMBA and 7-CMBA,^{8,21} are predicted to be the ultimate electrophilic and carcinogenic species that account for PAH carcinogenicity.^{2,3} We therefore deemed it important to gain an understanding of the reactivity of such compounds as revealed by MS even under thermal conditions in the ESI gas phase.

The 7-SMBA fragments and their structural interpretations disclosed that the even-electron 7-SMBA anion is capable of certain unusual ion transitions, some of them disallowed by the exception-prone even-electron rule^{22–25} as summarized in Fig. 12. Using the positive mode, we observed the benzylic cation at m/z 255 by loss of the sulfate dianion SO_4^{2-} (Fig. 4). However, by negative mode fragment ion analysis, rather than m/z 48 for a doubly charged anion, or m/z 97 for a monoprotonated sulfate, we observed m/z 96 as the principal fragment ion (Fig. 2(B)), indicating that 7-SMBA and presumably related benzylic sulfate esters are capable of generating the sulfate radical anion. Since this involves generation of an OE species, it would be considered disallowed, as opposed to the release of H_2SO_4 , SO_4^{2-} , HSO_3^- and SO_3 , all of which have precedents from organic sulfates described in the literature.^{26–32} The m/z 271 7-HMBA anion generated by release of SO_3 is allowed, but loss of a methyl radical to account for m/z 256 should probably be considered less likely. However, such methyl loss is a minor ion transition and therefore perhaps with good reason.

As mentioned, organic sulfates generally release stable even-electron moieties in MS experiments when observed, although there have been situations in which loss of the sulfate is not observed directly or indirectly.^{33,34} Although the sulfate radical anion is an OE species that is being studied under various conditions,^{35–38} generally from photolysis of $\text{S}_2\text{O}_8^{2-}$, to the best of our knowledge this is the first reported generation of this species from an organic sulfate. It is our belief that this is facilitated in 7-SMBA through radical delocalization between the extended π -orbital system and the benzylic carbon, but this remains to be proven.

Facile generation of a 7-SMBA photooxide was not particularly surprising, since such structures have been described for polyarenes since the 1970s.³⁹ We were interested, however, that this compound's fragment ion spectrum (Fig. 3) demonstrated, first, reversibility for the addition of oxygen, presumably as O_2 , and second, new routes for fragmentation, particularly release of naphthalenic residues, in comparison with the more stable 7-SMBA parent structure (Fig. 2).

The propensity of sulfate to act as an anionic leaving group accounts for the identification of an m/z 255 cation by ESI(+)-MS (Fig. 4), equivalent to the DNA-reactive carbonium ion capable of generating adducts with DNA *in vivo*.⁴⁰ The ability of 7-SMBA to generate this carbonium ion is fairly reasonable at room temperature, yet diminishes with moderately increased temperature as disclosed by the stability study displayed in Fig. 5.

The apparent proton rearrangements of carbonium ions during electrospray were an unexpected finding (Fig. 6). Based on studies of the halide derivatives, we concluded that reactions resulting from such rearrangements appear to depend at least initially on an induced acidity at the C-12 methyl group, and measurement of gas-phase acidity has been enabled primarily by MS, with which Gal *et al.*⁴¹ claim thousands of accurate measurements have been achieved. Suzuki and Tanaka⁴² have recently demonstrated exceptional acidity for the 9-methyl protons of the quaternary amine 9,10-dimethylacridinium chloride:

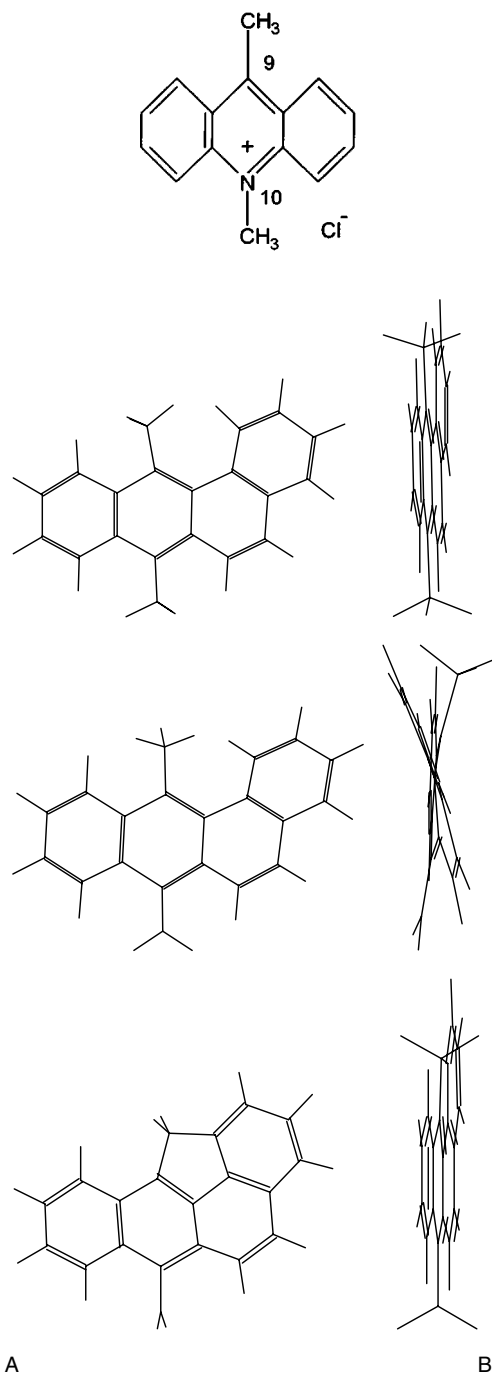


Figure 11. Hyperchem-optimized molecular stick figures for neutral DMBA (top), the 7-methylene-12-methylIBA carbocation derived from 7-IMBA or 7-SMBA (middle) and the ring-cyclized derivative of the 7-methylene-12-methylIBA carbocation with cyclization between carbons 1 and 12 and carbocation at C-7 (bottom). Structures were derived by utilization of semi-empirical AMBER quantum chemical calculation based on an initial charge of +1 on the methylene group (middle and bottom structures). (A) View from top of plane; (B) edge-on view from right side of A.

The acidity was demonstrated by rapid exchange with deuterium atoms as monitored by ^1H NMR spectroscopy with low energy barriers to dissociation. Structural studies showed a dependence on direct methyl substitution of the 9-methylacridine ring system at the 10-position for acidity.

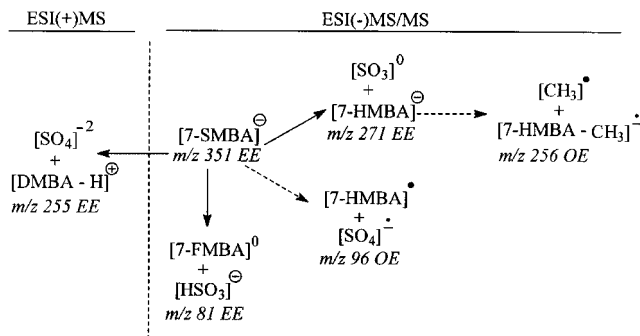


Figure 12. Summary of 7-SMBA ion transitions as revealed by ESI-MS, either positive (left) or negative mode (right). Even-electron (EE) and odd-electron (OE) species are labeled, and dotted arrows represent exceptions to the even-electron rule.^{22–25} There is literature support for the $\text{SO}_4^{\bullet-}$ radical anion;^{35–38} however, generation of m/z 256 by loss of a methyl radical seems less well supported.

Neither 9-methylacridine nor 9-ethylacridinium chloride evidenced the same capability, while thermodynamics greatly favored dissociation from 9-methylacridinium chloride relative to methyl isomers at position 1, 2, 3 or 4. In our opinion, similar considerations are apt to apply to 7-SMBA and its relatives.

Faigl *et al.*⁴³ measured similar benzylic proton acidity, specifically in halogenated toluene isomers with the exception of *p*-fluorotoluene. It is likely that acidity at the 7-SMBA 12-methyl group may also be a consequence of electron donor/attractor dualism, since Faigl *et al.* pointed out the acidity inherent in *p*-methoxytoluene benzylic protons. This property is likely to have been enhanced by collision-induced dissociation (CID), and Fleurat-Lessard *et al.*⁴⁴ noted differences in PAH proton transfers depending on structure, as did Arakawa *et al.*⁴⁵. Cardoso *et al.*⁴⁶ also described gas-phase deprotonation of arylalkylamines during negative mode CID, and suggest that such proton loss occurs at benzylic positions with H_2O as ionizing reagent. A 7-SMBA 12-position carbanion presumably would provide impetus for nucleophilic attack at the adjacent 1-position resulting in a cyclopentenyl ring.

The halo compounds support these inferences, both by their acidity to give directly visible anions by ESI(–)-MS (Figs 7 and 8) and by 7-IMBA's generation of a ring-cyclized variant under high-temperature effects of GC (Fig. 10). It is interesting that only the chloromethyl compounds readily formed dimeric complexes, which are presumably non-covalent, with one of the pair of molecules needing to lose a proton to provide a negative charge. This may well be an instrumental artifact, but nonetheless is of interest in establishing the relative acidity of these compounds. We assume loss of a proton at the 12-methyl position for 7-CMBA in analogy with the sulfate ester as gleaned from consideration of 9,10-dimethylacridinium (see above). 7-CBA is less obvious, in contrast, unless one invokes the possibility of abstraction of the 12-position proton itself.

An unusual aspect of the proton transfers evidenced by the data (Figs 11 and 12, Table 1) resided in the ability of moderate heat exposure to modulate the properties

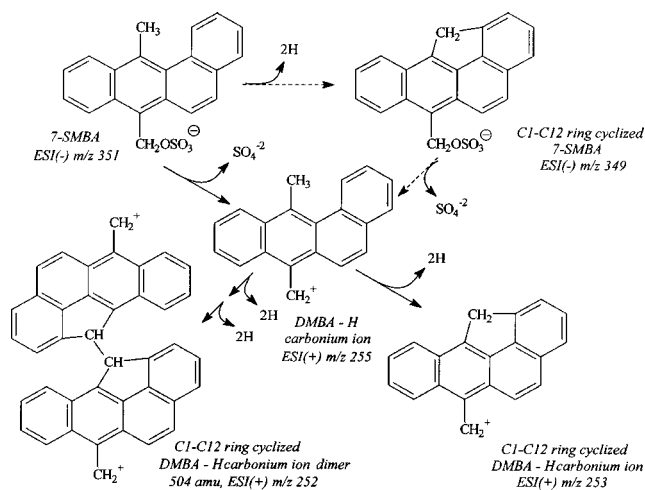


Figure 13. Formal summary of proposed routes from 7-SMBA to ESI(+)-MS-visualizable carbonium ions. Dotted line arrows indicate less likely pathways. 7-SMBA (upper left) loses sulfate to give the central carbonium ion, labeled 'DMBA - H' accounting for m/z 255 (Figs 4 and 5). C-1-C-12 cyclization then provides the 2 Da-less 'C-1-C-12 ring cyclized DMBA - H carbonium ion' (lower right) accounting for m/z 253 (Figs 6 and 9). The alternative path requiring cyclization prior to sulfate release (upper right) is unsupported by lack of evidence of m/z 349 (Fig. 2(A)). The central carbonium ion is proposed to undergo dimerization with loss of ≥ 4 Da to give a dicationic species 504 Da in size, to account for m/z 252, and possibly 250 (Fig. 6), an event more likely with higher carbonium ion concentrations, i.e. without thermal degradation. One such possible dimeric species is shown.

of the m/z 255 carbonium ion. Specifically, 7-SMBA m/z 255 generated the principal high molecular mass ions m/z 252 and 250 without heating and m/z 255 and 253 with heating (Fig. 6). The latter attribute was matched by the behavior of 7-IMBA (Fig. 9). The m/z 255 and 253 ions were not difficult to rationalize given their apparent abilities to give up sulfate or cyclize and give up sulfate, with the cyclization due to induced acidity at C-12 thereby enabling nucleophilic attack at C-1. However, the even-number masses m/z 252 and 250 posed more of a problem. One explanation consistent with the observed rapid diminution of carbonium ion populations on application of heat (Fig. 5) would invoke covalent intermolecular complexation to give species capable of supporting double cationic charges. An example of such thinking is summarized in the general scheme in Fig. 13, which summarizes proposed routes to 7-SMBA-derived carbonium ions. In addition to giving a possible example of a dimeric dication, Fig. 13 indicates that, since neither the ring-cyclized sulfate ester nor duplex sulfate ester m/z 349 or 348 were observed (cf. Fig. 2), it stands to reason that the cyclization or dimerization and the discharge of SO_4^{2-} are likely to be concerted reactions. Further loss of 2H to a bridging ethylene function could account for m/z 250 and offer the dimer kinship to coupled ring systems with overcrowded ethylenes.⁴⁷ This in turn may relate such coupled products to certain non-alternant buckminsterfullerene intermediates with distinct non-planarity following pyrolysis.⁴⁸

The presence of a cyclopentenyl ring in an unsubstituted PAH does not in any way restrict its applicability to the Meso-region theory of PAH carcinogenesis. Non-alternant polycyclic fluoranthenes, for example, have been examined by Dewar PI molecular orbital calculations for reactive centers, and compounds such as benz[*a*]aceanthrylene attain predictable carcinogenic potential based on the presence of a single site of substitution, similar to benzo[*a*]pyrene.⁴ A 1-12 methylene-bridged variant of benz[*a*]anthracene, specifically 11*H*-benz[*bc*]aceanthrylene, should have a single preferred center for reactivity, and its 6-methyl derivative, equivalent to the cyclized structure in Fig. 10, is a known carcinogen.⁴⁹

In summary, the data suggest that 7-SMBA is capable of cleavage to release sulfate and a 7-methylene-supported carbonium ion (M_r 255), the properties of which under the right conditions include the loss of two H atoms to yield a C-1-C-12 ring-cyclized carbonium ion (m/z 253) while also enabling coupling reactions at the C-12 carbon. Coupling at the 12-methyl position of DMBA derivatives is also not necessarily a new finding, since similar coupling has been observed by Cavalieri's group in studies of the formation of DNA adducts by attack at nucleophilic functionalities.^{50,51} In addition, precursor compounds are likely to be capable of reversible reaction with atmospheric oxygen to provide stable photooxides.

REFERENCES

- Flesher JW, Sydnor KL. Carcinogenicity of derivatives of 7,12-dimethylbenz[*a*]anthracene. *Cancer Res.* 1971; **31**: 1951.
- Flesher JW, Horn J, Lehner AF. Molecular modeling of carcinogenic potential in polycyclic hydrocarbons. *J. Mol. Struct. (Theochem)* 1996; **362**: 29.
- Flesher JW, Myers SR. Rules of molecular geometry for predicting carcinogenic activity of unsubstituted polynuclear aromatic hydrocarbons. *Teratogenesis Carcinogenesis Mutagenesis* 1991; **11**: 41.
- Flesher JW. Complete carcinogenic potential of polycyclic fluoranthene hydrocarbons in relation to their center or centers of highest electron density. *Polycycl. Arom. Compd.* 1994; **5**: 59.
- Lehner AF, Horn J, Flesher JW. Benzylic carbonium ions as ultimate carcinogens of polynuclear aromatic hydrocarbons. *J. Mol. Struct. (Theochem)* 1996; **366**: 203.
- Mandel HG. Pathways of drug biotransformation: biochemical conjugations. In *Fundamentals of Drug Metabolism and Drug Disposition*, La Du BN, Mandel HG, Way EL (eds). Robert E. Krieger: Huntington, NY, 1971; chapt. 10, 149.
- Banoglu E. Current status of the cytosolic sulfotransferases in the metabolic activation of promutagens and procarcinogens. *Curr. Drug Metab.* 2000; **1**: 1.
- Surh YJ, Liem A, Miller JA, Tannenbaum SR. 5-Sulfoxymethylfurfural as a possible ultimate mutagenic and carcinogenic metabolite of the Maillard reaction product, 5-hydroxymethylfurfural. *Carcinogenesis* 1994; **15**: 2375.
- Flesher JW, Soedigdo S, Kelley DR. Syntheses of metabolites of 7,12-dimethylbenz[*a*]anthracene, 4-hydroxy-7,12-dimethylbenz[*a*]anthracene, 7-hydroxymethyl-12-methylbenz[*a*]anthracene, their methyl ethers, and acetoxy derivatives. *J. Med. Chem.* 1967; **10**: 932.
- Flesher JW, Horn J, Lehner AF. 7-Sulfoxymethyl-12-methylbenz[*a*]anthracene is an ultimate electrophilic carcinogenic form of 7-hydroxymethylbenz[*a*]anthracene. *Biochem. Biophys. Res. Commun.* 1997; **231**: 712.
- Sandin RB, Fieser LF. Synthesis of 9,10-dimethyl-1,2-benzanthracene and of a thiophene isolog. *J. Am. Chem. Soc.* 1940; **62**: 3098.

12. Pataki J, Wlos R, Cho YJ. Adrenocorticolitic derivatives of benz[a]anthracene. *J. Med. Chem.* 1968; **11**: 1083.
13. Klein CL, Stevens ED, Zacharias DE, Glusker JP. 7,12-Dimethylbenz[a]anthracene: refined structure, electron density distribution and endoperoxide structure. *Carcinogenesis* 1987; **8**: 5.
14. Surh Y-J, Blomquist JC, Liem A, Miller JA. Metabolic activation of 9-hydroxymethyl-10-methylanthracene and 1-hydroxymethylpyrene to electrophilic, mutagenic and tumorigenic sulfuric acid esters by rat hepatic sulfotransferase activity. *Carcinogenesis* 1990; **11**: 1451.
15. Watabe T, Ishizuka T, Isobe M, Ozawa N. A 7-hydroxymethyl sulfate ester as an active metabolite of 7,12-dimethylbenz[a]anthracene. *Science* 1982; **215**: 403.
16. Binder TP, Duffel MW. Sulfation of benzylic alcohols catalyzed by aryl sulfotransferase. *Mol. Pharmacol.* 1988; **33**: 477.
17. Surh Y-J, Blomquist JC, Miller JA. Activation of 1-hydroxymethylpyrene to an electrophilic and mutagenic metabolite by rat hepatic sulfotransferase activity. In *Biological Reactive Intermediates IV*, Witmer CM (ed). Plenum Press: New York, 1990; 383.
18. Ohta M, Fujii S, Nonaka Y, Okamoto M. Metabolism of 11-deoxycortisol by cytochrome P450 (11 beta): identification of reaction products by 1H-NMR and LC/MS-APCI method. *Endocr. Res.* 1995; **21**: 477.
19. Fukunaga K, Suzuki T, Takama K. Highly sensitive high-performance liquid chromatography for the measurement of malondialdehyde in biological samples. *J. Chromatogr.* 1993; **621**: 77.
20. Anstead GM, Kym PR. Benz[a]anthracene diols: predicted carcinogenicity and structure-estrogen receptor binding affinity relationships. *Steroids* 1995; **60**: 383, and references cited therein.
21. Enders N, Seidel A, Monnerjahn S, Glatt HR. Synthesis of 11 benzylic sulfate esters, their bacterial mutagenicity and its modulation by chloride, bromide and acetate anions. *Polycycl. Arom. Compd.* 1993; **3**: (Suppl.): 887.
22. Karni M, Mandelbaum A. The 'even-electron' rule. *Org. Mass Spectrom.* 1980; **15**: 53.
23. Brown RD, Harrison AG. Loss of methyl radical from some small immonium ions: unusual violation of the even-electron rule. *Org. Mass Spectrom.* 1981; **16**: 180.
24. Krauss D, Mainx HG, Tauscher B, Bischof P. Fragmentation of trimethylsilyl derivatives of 2-alkoxyphenols: a further violation of the 'even-electron rule'. *Org. Mass Spectrom.* 1985; **20**: 614.
25. Ceraulo L, Agozzino P, Ferrugia M, Lamartina L, Natoli MC. Studies in organic mass spectrometry. Part 9. Mass spectra of 9,10-disubstituted 2,3,6,7-tetraalkoxy-9,10-dihydroanthracenes: a remarkable loss of radicals from even-electron ions. *Org. Mass Spectrom.* 1991; **26**: 279.
26. Tadano-Aritomi K, Kubo H, Ireland P, Okuda M, Kasama T, Handa S, Ishizuka I. Structural analysis of mono- and bis-sulfated glycosphingolipids by negative liquid secondary ion mass spectrometry with high- and low-energy collision-induced dissociation. *Carbohydr. Res.* 1995; **273**: 41.
27. Pan JF, Yu C, Zhu DY, Zhang H, Zeng JF, Jiang SH, Ren JY. Identification of three sulfate-conjugated metabolites of berberine chloride in healthy volunteers' urine after oral administration. *Acta Pharmacol. Sin.* 2002; **23**: 77.
28. Gunay NS, Tadano-Aritomi K, Toida T, Ishizuka I, Linhardt RJ. Evaluation of counterions for electrospray ionization mass spectral analysis of a highly sulfated carbohydrate, sucrose octasulfate. *Anal. Chem.* 2003; **75**: 3226.
29. Nemeth-Cawley JF, Karnik S, Rouse JC. Analysis of sulfated peptides using positive electrospray ionization tandem mass spectrometry. *J. Mass Spectrom.* 2001; **36**: 1301.
30. Siegel MM, Tabei K, Kagan MZ, Vlahov IR, Hileman RE, Linhardt RJ. Polysulfated carbohydrates analyzed as ion-paired complexes with basic peptides and proteins using electrospray negative ionization mass spectrometry. *J. Mass Spectrom.* 1997; **32**: 760.
31. McClellan JE, Costello CE, O'Connor PB, Zaia J. Influence of charge state on product ion mass spectra and the determination of 4S/6S sulfation sequence of chondroitin sulfate oligosaccharides. *Anal. Chem.* 2002; **74**: 3760.
32. Rondeau D, Bouchoux G, Vogel R, Muller E. Electrospray and chemical ionization mass spectrometry of di-n-butyl sulfate. Unimolecular chemistry of its protonated form and quantification method by liquid chromatography/electrospray ionization tandem mass spectrometry. *Rapid Commun. Mass Spectrom.* 2000; **14**: 1410.
33. Ikegawa S, Yanagihara T, Murao N, Watanabe H, Goto J, Niwa T. Separatory determination of bile acid 3-sulfates by liquid chromatography/electrospray ionization mass spectrometry. *J. Mass Spectrom.* 1997; **32**: 401.
34. Mitamura K, Nagaoka Y, Shimada K, Honma S, Namiki M, Koh E, Mizokami A. Simultaneous determination of androstenediol 3-sulfate and dehydroepiandrosterone sulfate in human serum using isotope diluted liquid chromatography-electrospray ionization-mass spectrometry. *J. Chromatogr. B* 2003; **796**: 121.
35. Yu X-Y, Bao Z-C, Barker JR. Free radical reactions involving Cl^\bullet , $\text{Cl}_2^{-\bullet}$, and $\text{SO}_4^{-\bullet}$ in the 248 nm photolysis of aqueous solutions containing $\text{S}_2\text{O}_8^{2-}$ and Cl^- . *J. Phys. Chem. A* 2004; **108**: 295.
36. Madhavan V, Levanon H, Neta P. Decarboxylation by sulfate(1-) radical. *Radiat. Res.* 1978; **76**: 15.
37. Luke TL, Mohan H, Manoj VM, Manoj P, Mittal JP, Aravindakumar CT. Reaction of sulfate radical anion ($\text{SO}_4^{-\bullet}$) with hydroxy- and methyl-substituted pyrimidines: a pulse radiolysis study. *Res. Chem. Intermed.* 2003; **29**: 379.
38. Galimova DI, Teregulova AN, Zapolskikh VV, Safiullin RL. Reaction kinetics of anion-radical $\text{SO}_4^{-\bullet}$ with C—H bonds of cyclic organic compounds. *Bashk. Khim. Zh.* 2001; **8**: 41.
39. Birks JB. The triplet state. In *Photophysics of Aromatic Molecules*. Wiley-Interscience: New York, 1970; 193.
40. Vadhanam MV, Horn J, Flesher JW, Gupta RC. Detection of benzylic adducts in DNA and nucleotides from 7-sulfooxymethyl-12-methylbenz[a]anthracene and related compounds by ^{32}P -postlabeling using new TLC systems. *Chem.-Biol. Interact.* 2003; **146**: 81.
41. Gal JF, Maria PC, Raczynska ED. Thermochemical aspects of proton transfer in the gas phase. *J. Mass Spectrom.* 2001; **36**: 699.
42. Suzuki H, Yasutaka T. An unusually acidic methyl group directly bound to acridinium cation. *J. Org. Chem.* 2001; **66**: 2227.
43. Faigl F, Marzi E, Schlosser M. Enhancement of benzylic basicity by a fluorine substituent at the para-position: a case of lone pair/lone pair repulsion. *Chem. Eur. J.* 2000; **6**: 771.
44. Fleurat-Lessard P, Pointet K, Milliet A. Contrasting behavior of tetracene and perylene in collision-induced dissociation: a theoretical interpretation. *J. Mass Spectrom.* 1999; **34**: 768.
45. Arakawa R, Kobayashi M, Nishimura T. High-energy collision-induced dissociation of small polycyclic aromatic hydrocarbons. *J. Mass Spectrom.* 2000; **35**: 178.
46. Cardoso AM, Alexandre SM, Barros CM, Correia AJ, Nibbering NM. Gas-phase deprotonation of arylalkylamine. A collision-induced dissociation study. *Rapid Commun. Mass Spectrom.* 1999; **13**: 1885.
47. Agranat I, Cohen S, Isaksson R, Sandstroem J, Suissa MR. Static and dynamic stereochemistry of a chiral, doubly bridged 9,10-diphenylanthracene from a stereospecific polycyclic aromatic dicarbonyl coupling. *J. Org. Chem.* 1990; **55**: 4943.
48. Rabideau PW, Sygula A. Buckybowls: polynuclear aromatic hydrocarbons related to the buckminsterfullerene surface. *Acc. Chem. Res.* 1996; **29**: 235.
49. Dunlap CE, Warren S. Carcinogenic activity of some new derivatives of aromatic hydrocarbons. II. Compounds related to 1,2-benzanthracene. *Cancer Res.* 1946; **6**: 454.
50. Devanesan PD, RamaKrishna NV, Padmavathi NS, Higginbotham S, Rogan EG, Cavalieri EL, Marsch GA,

- Jankowiak R, Small GJ. Identification and quantitation of 7,12-dimethylbenz[*a*]anthracene–DNA adducts formed in mouse skin. *Chem. Res. Toxicol.* 1993; **6**: 364.
51. Todorovic R, Ariese F, Devanesan P, Jankowiak R, Small GJ, Rogan E, Cavalieri E. Determination of benzo[*a*]pyrene– and 7,12-dimethylbenz[*a*]anthracene–DNA adducts formed in rat mammary glands. *Chem. Res. Toxicol.* 1997; **10**: 941.
52. Horn J, Flesher JW, Lehner AF. The metabolism of formyl-substituted benzanthracenes to hydroxymethyl metabolites in rat liver in vitro and in vivo. *Chem.–Biol. Interact.* 2003; **145**: 17.
53. Surh YJ. Bioactivation of benzylic and allylic alcohols via sulfonation. *Chem.–Biol. Interact.* 1998; **109**: 221.